

Dimensionality crossover induced by a magnetic field in thin metallic films

Z. Ovadyahu

Department of Physics, Ben-Gurion University of the Negev, 84120 Beer-Sheva, Israel

Yuval Gefen* and Yoseph Imry

School of Physics and Astronomy, Tel-Aviv University, 69978 Tel-Aviv, Israel

(Received 7 December 1984)

The field dependence of the magnetoconductance in finite-geometry samples is analyzed within the framework of the localization theory. It is found that for high magnetic fields the magnetoconductance acquires the functional field dependence characteristic of a three-dimensional system. This is so even when the inelastic mean free path is much larger than the sample thickness and when the zero-field transport properties of the system are two dimensional in character. The crossover point is obtained once the radius of the Landau level becomes smaller than the sample thickness for both the parallel and the perpendicular field orientations. These theoretical considerations are borne out by experiments on indium oxide films.

I. INTRODUCTION

The electronic conduction and its magnetic-field dependence in disordered conductors¹ can give information concerning the role of Anderson localization as well as electron-electron interactions²⁻⁹ in such systems. These effects are expected to depend on the effective dimensionality of the system and are known to be different in three-dimensional (3D) as compared with two-dimensional (2D) systems.¹⁰⁻²¹ In this connection one is faced with the question of what determines the effective dimensionality of a given system. This paper deals with some theoretical and experimental aspects of this question with a special emphasis on the 3D→2D crossover. Similar considerations should apply for the crossover to one-dimensional (1D) behavior²²⁻²⁵ which will not be specifically addressed here. These crossovers are governed by the interplay between the relevant lengths in the problem: the inelastic diffusion length l_T , the magnetic length $l_H \equiv (\hbar c / eH)^{1/2}$, and the sample thickness d . We shall present the theoretical analysis in the context of the weak localization theory which seems to give an adequate description of our experimental results discussed later. Similar consideration should apply when the interaction contribution is considered with l_T replaced by $(\hbar D / kT)^{1/2}$ (see Sec. II for definitions).

In zero field, the 3D→2D crossover in the conductivity σ is expected to occur when l_T becomes comparable with d . This question has recently been addressed by Berggren.²⁶ Our theoretical considerations are presented in the first part of Sec. II. In the second part of Sec. II we discuss the analogous crossover induced by a perpendicular magnetic field at constant temperature. We find²¹ that even for films that are 2D with respect to their $\sigma(T)$ behavior ($d \ll l_T$) a 3D behavior of the magnetic resistance (MR) is obtained once the applied field is strong enough to make l_H smaller than d . The result is qualitatively similar to that obtained by Al'tshuler and Aronov²⁷ for the parallel field case where the notation of a cross-

over to 3D is intuitively more transparent.

The theoretical considerations of Sec. III are compared in Sec. IV with experiments performed on $\text{In}_2\text{O}_{3-x}$ films of various thicknesses. The experimental results confirm the qualitative features of the expected field-induced crossover, in particular, the correlation between the crossover field and d is well established. In addition, we find that the logarithmic slope of the MR for a sufficiently large parallel field is twice as large as that for a perpendicular one (for $d < l_H < l_T$). This is in agreement with the theoretical predictions of Ref. 27.

II. THEORY OF 2D-3D CROSSOVER

In general, the conductivity $\sigma(H, T)$ in magnetic field H and temperature T may be written as

$$\sigma(H, T) = \sigma_0 + \sigma_1(H, T), \quad (1)$$

where σ_0 is the Boltzmann part of the conductivity

$$\sigma_0 = ne^2\tau/m, \quad (2)$$

n , m , and τ being the electron density, effective mass, and the electron's relaxation time due to elastic scattering, respectively. σ_1 is the anomalous part. We consider a three-dimensional sample of a finite width, d . To obtain the temperature dependence of σ , when the magnetic field is zero, the correction to the conductivity is given by^{2,6}

$$\sigma_1(0, T) = \frac{e^2}{2\pi^2\hbar d} \sum_{n=0}^{Ad/2\pi a} \ln \left[\frac{a^2}{2D\tau_{in}} + 2\pi^2(a/d)^2 n^2 \right], \quad (3)$$

where a is some microscopic length (which is in this case the elastic mean free path), D is the diffusion coefficient, and τ_{in} is the inelastic or phase breaking time, $(2D\tau_{in})^{1/2} = l_T$. We assume $a \ll l_T, d$. Here $\hbar A/a$ is the upper cutoff in momentum. The two-dimensional (2D) result is obtained from Eq. (3) by taking only the term with $n=0$,

$$\begin{aligned}\sigma_1^{2D}(0, T) &= \frac{e^2}{2\pi^2\hbar d} \ln \left[\frac{a^2}{2D\tau_{in}} \right] \\ &= \frac{2e^2}{\pi\hbar d} [\ln(a/d) + \ln(d/l_T)].\end{aligned}\quad (4)$$

The 3D limit is obtained by replacing the summation in Eq. (3) by an integral. This is allowed when the inelastic length ("Thouless length"), l_T , is much smaller than d , $d \gg l_T$. The result of the integration is²⁸

$$\begin{aligned}\sigma_1^{3D}(0, T) &= \frac{A}{2\pi^3} \frac{e^2}{\hbar a} (\ln A - C) + \frac{e^2}{4\pi^2\hbar(D\tau_{in})^{1/2}} \\ &\quad \times \left[1 + O \left[\frac{a}{(D\tau_{in})^{1/2}} \right] \right].\end{aligned}\quad (5)$$

The first term renormalizes the "bare" conductivity, σ_0 , C is a numerical constant of order unity (for $\ln A = C$ this correction vanishes). We leave open the question of the observability of this correction. A plot of $\sigma_1(0, T)$ [Eq. (3)] versus $d/(D\tau_{in})^{1/2}$ is shown in Fig. 1. For $d/(D\tau_{in})^{1/2} \ll 1$ we recover the 2D behavior [Fig. 1(a)]. For $d/(D\tau_{in})^{1/2} \gg 1$ we find a linear dependence on $1/l_T$ [Fig. 1(b)] as expected. The corresponding behavior for a three-dimensional system [i.e., $d \rightarrow \infty$, see Eq. (5)], is shown by a dashed line. Note that when $l_T \ll d$ one still finds a correction factor with respect to the "ideal" 3D result. The difference between the finite thickness sample and the "true" 3D case is essentially due to the $n=0$ term (i.e., the 2D contribution) in Eq. (3). This difference is practically constant (in fact it varies logarithmically) as a function of l_T and therefore the relative correction goes to zero. Such deviations from the 3D behavior, which exist even for $d \gg l_T$, should in principle be observable in the experiments. Note also that the variation of σ_1 is smooth and no sharp changes in slope²⁶ are obtained. We emphasize that the above-mentioned corrections are not just functions of d/l_T .

The 2D to 3D crossover occurs at $d/l_T \sim 1$. This crossover is determined in theory, as well as experimentally, by the change of slope of σ_1 , from linear to logarithmic behavior. We emphasize that it should *not* be determined by, say, the condition that σ_1 and σ_1^{2D} are comparable. This latter criterion, which yields a different relation between d and l_T at the crossover, cannot be simply related to experiment.

We now introduce a magnetic field.^{10,21} The problem of magnetic field *parallel* to the surface has been already discussed by Al'tschuler and Aronov.²⁷ Here we shall consider the problem of magnetic field *perpendicular* to

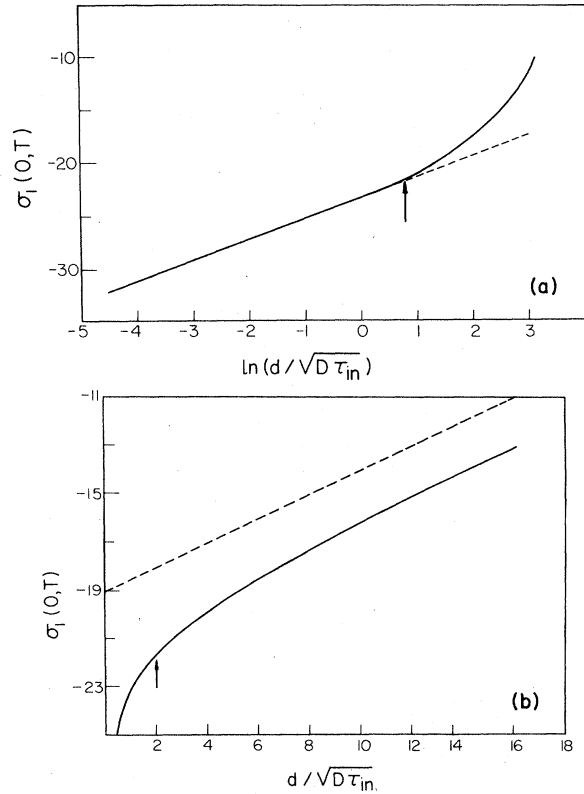


FIG. 1. Anomalous conductivity σ_1 , in units of $e^2/2\pi^2\hbar d$, as function of temperature, parametrized by d/l_T . (a) Using a logarithmic scale for d/l_T —on which σ_1 is linear for $d < (D\tau_{in})^{1/2}$ (2D case). (b) Same quantities on a linear scale; σ_1 is linear in $l_T^{-1/2}$ for $d \gg l_T$ (3D behavior). These calculations were done for films with $d/a=60$. In (a) and (b) the dashed line depicts the pure 2D and 3D behaviors, respectively.

the layer. In this case we write

$$\sigma_1(H, T) = \sigma_a(H, T) + \sigma_b(H, T). \quad (6)$$

σ_a is the "2D contribution" measured in $(\text{ohm cm})^{-1}$, and is equal to

$$\sigma_a(H, T) = -\frac{2e^2D}{\pi^2l_H^2\hbar d} \sum_{n=0}^{N_0} \frac{1}{4Dl_H^{-2}(n + \frac{1}{2}) + 1/\tau_{in}}, \quad (7)$$

where $l_H^2 = \hbar^2/m^2c^2$ is the square of the radius of the lowest ($n=0$) Landau orbital of an electron in a magnetic field H . We take $l_H \gg a$. The related cutoff parameter is $N_0 \sim l_H^2/a^2$. The second contribution in Eq. (6) is σ_b :

$$\sigma_b = -\frac{4e^2D}{\pi^2l_H^2\hbar d} \sum_{n'=1}^{Ad/2\pi a} \sum_{n=0}^{N_0} \frac{1}{4Dl_H^{-2}(n + \frac{1}{2}) + D(2\pi n'/d)^2 - 1/\tau_{in}}. \quad (8)$$

The assumption in Eqs. (7) and (8) is that the magnetic field is weak enough so that the resulting modification of the one-particle states may be ignored in the disordered system.^{6,7} The magnetoconductivity (MC) $\Delta\sigma$, is defined

by

$$\Delta\sigma(H, T) \equiv \sigma_1(H, T) - \sigma_1(0, T). \quad (9)$$

The 2D part of the MC is^{3,5}

$$\begin{aligned} \Delta\sigma_a(H,T) &= \sigma_a(H,T) - \sigma_a(0,T) \\ &= \frac{e^2}{2\pi^2\hbar d} \left[\psi \left(\frac{l_H^2}{2l_T^2} + \frac{1}{2} \right) - \ln \left(\frac{l_H^2}{2l_T^2} \right) \right], \end{aligned} \quad (10)$$

where $\psi(z)$ is the digamma function.

In the weak-field (or high-temperature) limit ($l_H \gg l_T \gg a$), Eq. (10) reduces to

$$\Delta\sigma_a = \frac{e^2}{12\pi^2\hbar d} \left[\frac{l_T^4}{l_H^4} \right], \quad (11)$$

whereas the strong-field limit ($a \ll l_H \ll l_T$) yields

$$\Delta\sigma_a = \frac{e^2}{2\pi^2\hbar d} \left[-1.964 - \ln \left(\frac{l_H^2}{2l_T^2} \right) \right]. \quad (12)$$

We now consider the other contribution, σ_b . If we are allowed to replace the summation over wave vectors [first summation in Eq. (8)] by integration, we obtain the usual 3D results⁴

$$\Delta\sigma_b = \begin{cases} \frac{\sqrt{2}}{48} \frac{e^2}{\pi^2\hbar} \frac{l_T^3}{l_H^4}, & l_H \gg l_T \\ \frac{C_1 e^2}{2\pi^2\hbar l_H}, & l_H \ll l_T \end{cases} \quad (13a)$$

$$\Delta\sigma_b = \begin{cases} \frac{C_1 e^2}{2\pi^2\hbar l_H}, & l_H \ll l_T \end{cases} \quad (13b)$$

where

$$C_1 = \sum_{n=0}^{\infty} \left[2(\sqrt{n+1} - \sqrt{n}) - \frac{1}{(n + \frac{1}{2})^{1/2}} \right] \approx 0.605.$$

In analogy with the above discussion of the temperature-dependent conductivity, the 2D to 3D crossover in the presence of a magnetic field should be found by considering the slope of the MC.²⁹

We now consider two cases

(a) $l_T \ll l_H$. We find from Eqs. (11) and (13a) that the condition for crossover is

$$l_T \approx d, \quad (14a)$$

as in the zero-field case.

(b) $l_T \gg l_H$. We find from Eqs. (12) and (13b) that the crossover occurs at

$$l_H \approx d. \quad (14b)$$

Note that this strong-field (or low-temperature) crossover occurs at an H value which is independent of temperature.

Figure 2 shows the H dependence of the MC [Eq. (9)] for three values of d/l_T (which is the parameter determining the effective dimensionality for $\sigma_1(l,T)$). In the two "thin" sample cases [Figs. 2(a) and 2(b)] shown, the behavior of the MC merges with the 2D one for $d/l_H \ll 1$ and becomes essentially parallel to the 3D one for $d/l_H \gg 1$. In the thick one [Fig. 2(c)], the behavior is almost indistinguishable from the 3D one [Eq. (13)]. All these results are in agreement with our above discussion. We note also, as discussed before, a difference between the value of the full MR and the 3D contribution. This difference appears to be roughly a coefficient multiplying

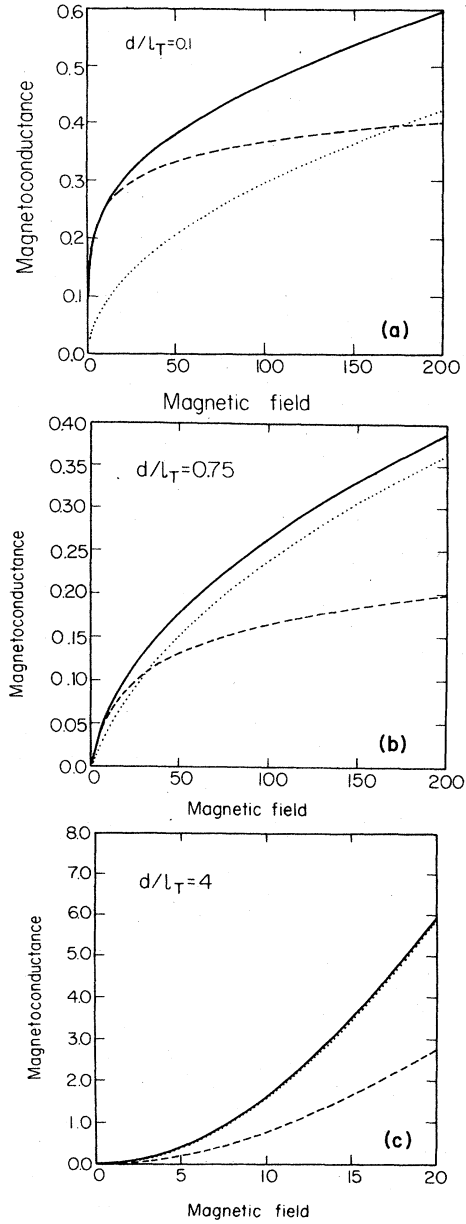


FIG. 2. Magnetoconductance in units of e^2/\hbar for various films as a function of the magnetic field in units of $c\hbar/ed^2$. Solid curves, numerical calculation; dotted curves, 3D contributions $\Delta\sigma_b$ [Eqs. (8) and (13)]; dashed curves, the pure 2D contribution $\Delta\sigma_a$ [Eq. (7) and (10)]. The calculations were done for three thicknesses: (a) $d/l_T=0.1$ (2D-like behavior); (b) $d/l_T=0.75$ (2D intermediate behavior); (c) $d/l_T=4$ (3D-like behavior).

the 2D contribution. The coefficient is of the order of 40% for the thinnest case, and decreases monotonically with increasing thickness. Thus, for very thin samples it takes a much larger field than that for which $l_H \sim d$ to establish 3D behavior not only with respect to the slope but also for the value of $\Delta\sigma(H,T)$.

In order to gain some physical insight into the problem of dimensional crossover in the MC, let us consider an electron wave packet which develops in time in the pres-

ence of some magnetic field. The length l_H , as well as l_T , plays the role of a characteristic scale for the system to lose its $H=0$, $T=0$ quantum coherence. Thus if $\bar{l} \equiv \min(l_H, l_T) \ll d$, the finite thickness of the system is not felt by the propagating wave packet and the behavior is, to a leading order, 3D. Once $\bar{l} \sim d$, a crossover to a 2D behavior takes place. Alternatively, one may say that the relevant wave vector, appearing in the expression for σ_1 , should satisfy $|q| < 1/\bar{l}$. Since q is quantized ($q=0, \pm 2\pi/d, \dots$), $\bar{l} \gg d$ implies that only the $q=0$ term (i.e., the 2D contribution) should be taken into account. The condition for crossover from 2D to 3D behavior in the *parallel* field case was found in Ref. 27 to be similar to the one we find here. In the parallel field case the physical picture is more obvious since the motion due to the field is perpendicular to the surface of the film. A point to be emphasized is that in the parallel field case of Ref. 27, the slope of the MC versus $\ln H$ in the range $d \ll l_H \ll l_T$ is *twice* that of the perpendicular field case [compared Eq. (12) with Eq. (9) of Ref. 27].

Finally, we would like to emphasize that the “weak-scattering” ($k_f l \gg 1$) theory discussed above is expected to apply only when the correlation length is irrelevant. This is the usual case when $k_f l$ and l_T are sufficiently large. However, when the metal-insulator transition is approached and ξ becomes appreciable, it may be necessary to modify the theoretical treatment given above.

III. EXPERIMENTAL TECHNIQUES

In $\text{In}_2\text{O}_{3-x}$ samples were prepared by *e*-gun deposition of pure (99.997%) hot-pressed indium-oxide powder. Microscope glass slides held at $\sim 150^\circ\text{C}$ were used as substrates and the desired geometry were obtained by the use of appropriate stainless-steel masks. Further details of preparation and samples characterization are given elsewhere.³⁰ For completeness we give here details of two of the features that may be of particular relevance to the present study. The thickness of the films was measured, *in situ*, with a quartz crystal which was periodically calibrated against a Tolanski interferometer. We estimate the uncertainty in absolute thickness determination to be $\pm 10\%$ and the relative uncertainty $\pm 5\%$. The other point is the surface roughness or the thickness variation of our films. Figure 3 is a high magnification TEM micrograph of a typical sample prepared with the prescribed³⁰ conditions. The surface roughness observed amounts to ± 20 Å, apparently independent of the total thickness. Since the thinnest film used in this study is ~ 350 Å, we feel that the physical thickness of our film is quite well defined. This fact may be crucial for the unambiguous observation of the 3D \rightarrow 2D crossover to be discussed below.

Conductivity measurements were performed as a function of field and temperature employing a standard dc four-terminal technique. The magnetic field was achieved by a conventional split-coil design magnet that could be rotated 360° relative to the sample's plane. Electrical contacts were soldered in the $\text{In}_2\text{O}_{3-x}$ samples with pure metallic indium, a method that in principle, might influence the magnetic field inhomogeneity at field smaller than

~ 300 Oe (which is for the critical field of indium in the superconductivity state). We did not detect, however, any spurious behavior at the field in question. Moreover, the data relevant to the field-induced crossover were taken at fields which are considerably higher than ~ 300 Oe. This is described in the next section.

IV. RESULTS AND DISCUSSION

In this section we describe and discuss the experimental results obtained for the resistance of the indium-oxide films as a function of field and temperature. Since in virtually all cases described below the fractional change of the resistance (with either field or temperature) is quite small, $\Delta\sigma/\sigma$ has essentially the same magnitude as $\Delta R/R$. It should be noted that the latter is used in this section.

Figures 4(a) and 4(b) depict the temperature dependence of several $\text{In}_2\text{O}_{3-x}$ films with thicknesses ranging between 350 to 1250 Å. These data were taken at a field of $\sim 2 \times 10^{-3}$ Oe (which was the residual field inside a double- μ -metal shield) and at electric fields of the order of 10^{-3} V/cm. We have not noticed any change, within our experimental error, in the resistivity at a constant temperature, in fields which were 1D times larger than those quoted. It is therefore believed that these measurements yield the “zero-field” resistivity as a function of temperature.

In each case, it is observed that there is a temperature, T_d , below which the film's resistance increases logarithmically with temperature. Above T_d the functional dependence of $R(T)$ takes on a different form, for example, $R(T) = R_0 = AT^{1/3}$ which is believed to be the resistivity versus temperature law in the microscopic (critical) 3D regime of this material. It is thus natural to associate

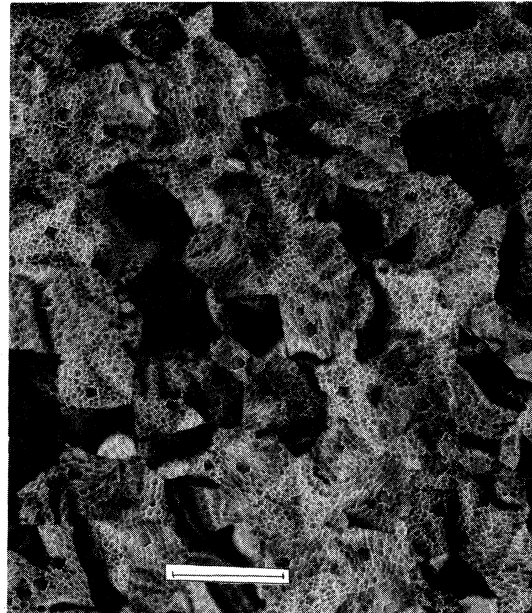


FIG. 3. Bright-field micrograph of a 300 Å $\text{In}_2\text{O}_{3-x}$ sample taken at a JEOL-100C transmission electron microscope. The black bar is equivalent to a length of 0.4 μm .

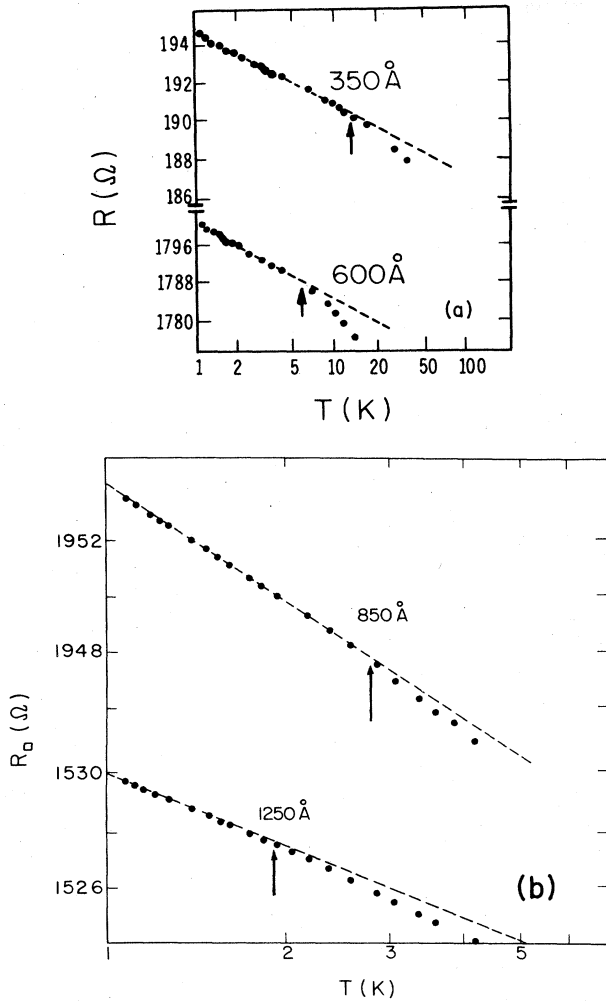


FIG. 4. Zero-field resistance versus temperature (on a logarithmic scale), for samples with various thicknesses (as indicated). In each case the 3D→2D crossover temperature, T_d , is marked by an arrow. Note the similarity between thinner samples (a) and the theoretical result [Fig. 1(a)]. It is seen that for the thicker samples (b), T_d occurs at progressively lower temperatures.

T_d with the 3D→2D crossover temperature. We note that such a procedure constitutes a valid measurement of l_T . It should be pointed out that measurements along these lines when compared with MR experiments seem to indicate³¹ that $l_T(T=T_d)=d$ within an uncertainty of $\pm 20\%$.

We turn now to the MR results of the four films described above. These are given in Figs. 5, 6(a), 6(b), and 7. The most obvious aspect of the data shown in these figures is the gradual decrease of anisotropy (i.e., the differences between the MR for parallel and perpendicular field orientations), for a given field and temperature, as the thickness increases. It can also be observed that this anisotropy decreases with temperature for a given sample at a constant magnetic field. This was first noted in Ref. 21. There are two interesting features in these results that we wish to discuss in some detail. The first concerns the

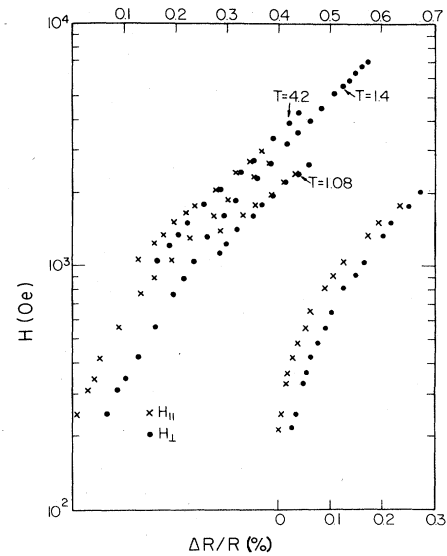


FIG. 5. Negative MR results for the 1250-Å sample measured at several temperatures below T_d for both field orientations. The two lowest curves show for comparison the full low-field behavior at 4.2 K. Note that while low-field anisotropy is significantly affected by temperature, the crossing field is not. It is interesting to note that this is so even in the temperature range where the film is effectively 3D.

asymptotic high-field logarithmic slopes of the parallel and perpendicular MR results. The theoretical expression for the MR in a parallel field is²⁷

$$\frac{\Delta R}{R} = \frac{e^2 R_{\square}}{2\pi^2 \hbar} \ln \left[\frac{d^2 l_T^2}{12 l_H^2} + 1 \right],$$

which reduces to

$$\frac{\Delta R}{R} \approx \frac{e^2 R_{\square}}{2\pi^2 \hbar} \ln \left[\frac{d^2 l_T^2}{12 l_H^4} \right] \quad (15)$$

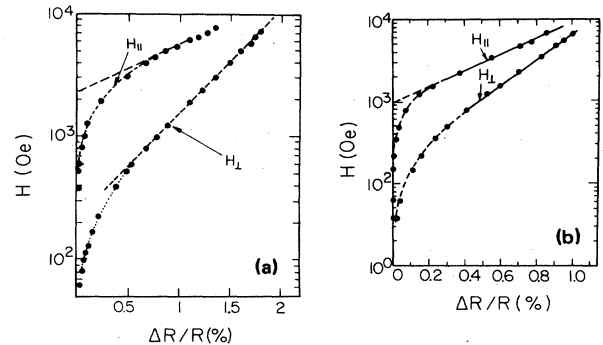


FIG. 6. Negative MR measured at 4.2 K in parallel and perpendicular field orientations (marked $H_{||}$ and H_{\perp} , respectively) for (a) 350-Å-thick and (b) 600-Å-thick samples. The dashed straight line on the parallel-field MR is used to define H_0 . Note (by reference to Fig. 4) that, in the absence of field, both samples are 2D in this temperature.

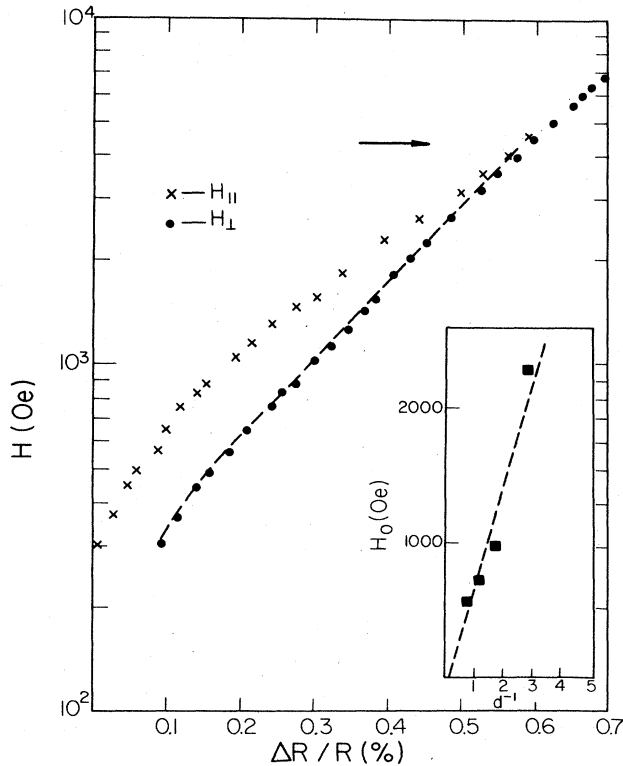


FIG. 7. Negative MR results in both fields orientations for a 850-Å film (measured at 1.4 K, where according to Fig. 4 the film is effectively 2D in zero field). The inset depicts H_0 (cf., e.g., Fig. 6) as a function of the inverse of the films thickness (in units of 10^5 cm^{-1}).

for magnetic fields so high that $l_H^2 \ll l_T d$. This should be compared with³

$$\frac{\Delta R}{R} \approx \frac{e^2 R_{\square}}{2\pi^2 \hbar} \ln \left[\frac{2l_T^2}{l_H^2} \right], \quad (16)$$

which is the analogous expression appropriate for the high-field ($l_H \ll l_T$) MR of a 2D film ($d \ll l_T$) whose plane is oriented perpendicular to the field. It is thus expected that the high-field 2D limit (i.e., $d \ll l_H \ll l_T$) will be reached first for the perpendicular orientation. Asymptotically, a logarithmic increase of the MR with field will be exhibited for both field orientations. Further, we can be seen by comparing Eqs. (15) and (16), the logarithmic slope of the MR for the parallel field is exactly twice that of the perpendicular one. The data for the 350- and 600-Å samples (Fig. 6) clearly demonstrate the above three features. The logarithmic slopes ratio for the 350-Å sample is 1.9 ± 0.1 , and it is 1.7 ± 0.1 for the 600-Å sample. We ascribe the difference from the ideal value of 2.0 to the finiteness of d/l_T . It would be of much interest to study the behavior of the thicker films in lower temperatures, where l_T is presumably larger, to verify this conjecture. The second point concerns the crossing of the MR curve for a parallel field with that of the perpendicular one. This should occur according to (15) and (16) for $l_H \sim (\sqrt{6}/12)d$ and is thus a purely geometrical condition. A similar condition might be derived from a quasiclassical description of the quasiparticle trajectory. One ex-

pects the MR to be isotropic once the time it “takes” the quasiparticle to diffuse a distance d exceeds the time to complete a full circle ($\sim \pi l_H$). Either way we have an easy to verify prediction—the curves should cross at a temperature-independent point and at fields that scale³² as d^{-2} . Comparing this with our data we find that this is indeed so, but the empirical proportionality constant is ~ 0.35 rather than the theoretical $\sqrt{6}/12$. The insensitivity of the crossing field to temperature is illustrated in Fig. 5. Another characteristic field that comes out of such considerations is obtained by extrapolating the asymptotical form of the MR for the parallel orientation to $\Delta R/R=0$ (see dashed lines in Fig. 6). From (15) it is seen that this field H_0 is defined by $dl_T = 2\sqrt{3}l_H^2$, which suggests a dependence of the form $H_0 \propto d^{-1}$ (with a temperature-dependent proportionality constant). We have attempted to see how this relationship fits our data in the inset of Fig. 7. This gives a reasonable curve and, in fact, the value of l_T obtained from the slope of these data, $\sim 1300 \text{ Å}$ at 4.2 K, agrees favorably with $l_T \sim 1000 \pm 100 \text{ Å}$ obtained elsewhere³¹ for the same films using two different methods.

From the experimental point of view it is easy to understand the field-induced crossover which seems to occur at or close to the point where $(\Delta R/R)_{H_{\perp}} = (\Delta R/R)_{H_{\parallel}}$. Clearly, (15) and (16) should be modified for fields higher than the crossing field since otherwise $(\Delta R/R)_{H_{\parallel}}$ will be larger than $(\Delta R/R)_{H_{\perp}}$ which would appear to conflict with the physical idea underlying (15) and (16). The natural solution is that both curves will deviate at this point from their $\ln H$ field-dependence characteristic of the 2D sample into the $H^{1/2}$ dependence expected in the 3D range. This indeed seems to be the case (Figs. 5 and 6) though our limited range of fields does not allow for a definitive functional dependence to be established. This analysis confirms the theoretical considerations of Sec. II according to which the 2D \rightarrow 3D crossover defined by the functional dependence on the field is essentially independent of temperature. At the same time some questions regarding the form of the 3D behavior are raised. For example, according to Kawabata⁴ in the pure 3D case the high-field regime has the universal feature that $\Delta\sigma(H, T) = 0.918\sqrt{H} \text{ mho cm}^{-1}$ (where H is in koe), regardless of material and temperature. Usually, this prediction is borne out by experiments performed on thick samples to within an order of magnitude,^{11,12} but conspicuous variations do occur. The experimental results for $\Delta\sigma/\sqrt{H}$ seem to indicate that temperature dependence cannot be neglected. Some of these discrepancies might be traced to other mechanisms not treated here such as spin-orbit coupling.³ However, the considerations made above suggest that in finite-geometry samples³² the “Kawabata’s number” $\Delta\sigma/\sqrt{H}$ will be temperature dependent to a significant degree simply through the “background contribution” of the 2D component (see Fig. 2). This may be of some relevance even for thick films where $d \gg l_T$ if an inherent structural anisotropy is present which is often the case in granular metal films.

Note added in proof. Dimensional crossover with magnetic fields has also recently been reported by P. Ohya,

M. Okamoto, and E. Otsukai, *J. Phys. Soc. Jpn.* **54**, 1041 (1985).

ACKNOWLEDGMENTS

The experimental work reported in this paper was performed at Brookhaven National Laboratory under the

auspices of the U. S. Department of Energy under Contract No. DE-AC02-76CH00016. Research at Tel-Aviv University was partially supported by the U. S.—Israel Binational Science Foundation (BSF), Jerusalem, Israel, and by the Israel Academy of Sciences and Humanities.

*Present address: Institute for Theoretical Physics, University of California, Santa Barbara, CA 23106.

¹E. N. Adams and T. D. Holstein, *J. Phys. Chem. Solids* **10**, 254 (1959).

²E. Abrahams, P. W. Anderson, D. C. Licciardello, and T. V. Ramakrishnan, *Phys. Rev. Lett.* **42**, 673 (1979); E. Abrahams and T. V. Ramakrishnan, *J. Non-Cryst. Solids* **35**, 15 (1980).

³S. Hikami, A. I. Larkin, and Y. Nagaoka, *Prog. Theor. Phys.* **63**, 707 (1980).

⁴A. Kawabata, *J. Phys. Soc. Jpn.* **49**, 628 (1980); **50**, 2461 (1980); *Solid State Commun.* **38**, 823 (1981).

⁵B. L. Altshuler, D. E. Khmel'nitzkii, A. I. Larkin, and P. A. Lee, *Phys. Rev. B* **22**, 5142 (1980).

⁶H. Fukuyama, in *Proceedings of the 4th International Conference on Electronic Properties of Two-Dimensional Systems, New Hampshire, August 1981*, edited by F. Stern (North-Holland, Amsterdam, 1982), p. 489.

⁷H. Fukuyama, Institute for Solid State Physics (University of Tokyo) Technical Report (Ser. H) No. 1304, 1983 (unpublished), and references therein.

⁸P. A. Lee and T. V. Ramakrishnan, *Phys. Rev. B* **26**, 4009 (1980).

⁹A. I. Larkin, *Pis'ma Zh. Eksp. Teor. Fiz.* **31**, 239 (1980) [*JETP Lett.* **31**, 219 (1980)].

¹⁰Y. Imry and Z. Ovadyahu, *J. Phys. C* **15**, L327 (1982).

¹¹T. Chui, P. Lindenfeld, W. L. Mclean, and K. Mui, *Phys. Rev. Lett.* **47**, 1617 (1981).

¹²Z. Ovadyahu, *Phys. Rev. Lett.* **52**, 569 (1984).

¹³G. Bergmann, *Phys. Rev. Lett.* **49**, 162 (1982).

¹⁴G. Bergmann, *Phys. Rev. Lett.* **48**, 1046 (1982).

¹⁵G. Bergmann, *Z. Phys.* **48**, 5 (1982).

¹⁶Y. Kawaguchi and S. Kawaji, *J. Phys. Soc. Jpn.* **48**, 699

(1980).

¹⁷J. M. Gordon, C. J. Lobb, and M. Tinkham, *Phys. Rev. B* **28**, 2046 (1983).

¹⁸R. A. Davies and M. Pepper, *J. Phys. C* **16**, L353 (1983).

¹⁹R. G. Wheeler, *Phys. Rev. B* **24**, 4645, (1981).

²⁰T. Ando, A. B. Fowler, and F. Stern, *Rev. Mod. Phys.* **54**, 437 (1982), and references therein.

²¹Z. Ovadyahu, S. Mohlecke, and Y. Imry, *Surf. Sci.* **113**, 544 (1982).

²²A. B. Fowler, A. Hartstein, and R. A. Webb, *Phys. Rev. Lett.* **48**, 196 (1982).

²³D. J. Bishop, R. C. Dynes, and D. C. Tsui, *Phys. Rev. B* **26**, 773 (1982).

²⁴R. G. Wheeler, K. K. Choi, A. Goel, R. Wisnieff, and D. E. Prober, *Phys. Rev. Lett.* **49**, 1674 (1982).

²⁵Z. Ovadyahu and Y. Imry, *J. Phys. C* (to be published).

²⁶K. F. Berggren, *J. Phys. C* **15**, L843 (1982).

²⁷B. L. Al'tshuler and A. G. Aronov, *Pis'ma Zh. Eksp. Teor. Fiz.* **33**, 515 (1981) [*JETP Lett.* **33**, 499 (1981)].

²⁸E. S. Gradshteyn and I. M. Ryzhik, *Tables of Integrals, Series and Products* (Academic, New York, 1985).

²⁹We emphasize that even in the "3D regime" the value of the MC will differ from that of an ideal 3D system with a correction due to the 2D term. It would be useful to verify this experimentally.

³⁰Z. Ovadyahu, B. Ovrin, and H. W. Kraner, *J. Electrochem. Soc.* **130**, 917 (1983).

³¹Z. Ovadyahu, *J. Phys. C* **16**, L845 (1983).

³²M. Ya. Azbel and V. G. Peschanskii, *Zh. Eksp. Teor. Fiz.* **49**, 532 (1965) [*Sov. Phys—JETP* **22**, 399 (1966)] have discussed related size effects in clean films.

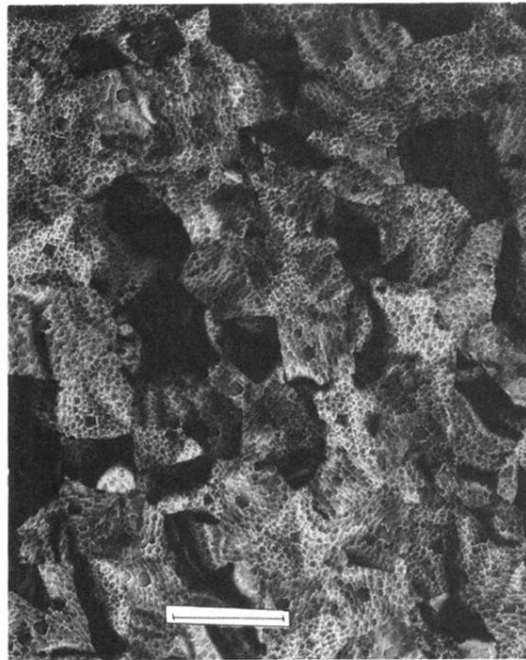


FIG. 3. Bright-field micrograph of a 300 Å $\text{In}_2\text{O}_{3-x}$ sample taken at a JEOL-100C transmission electron microscope. The black bar is equivalent to a length of 0.4 μm .